

Support Informations

Dithia[3.3]paracyclophane-Bridged Bimetallic Ruthenium Acetylide Complexes : Synthesis, Structures and Influence of transannular π - π interactions on Their Electronic Properties

Jianlong Xia*, Ya-Ping Ou, Di Wu, Guo-Jun Jin, Jun Yin, Guang-Ao Yu, Sheng Hua Liu*

Key Laboratory of Pesticide and Chemical Biology, Ministry of Education, College of Chemistry, Central China

Normal University, Wuhan 430079, P.R. China

*Corresponding Author, Email: chshliu@mail.ccnu.edu.cn (S. H. Liu) jianlongxia@gmail.com (J. Xia)

Table S1. Crystal data and structure refinement for **2** and **3**.

Figure S1. Cyclic voltammograms (CV) of complexes **2** and **3**.

Figure S2. IR spectra of **1**ⁿ⁺ (n = 0–2) collected during the oxidation titration with ferrocenium hexafluorophosphate([FcH][PF₆]).

Figure S3. UV/Vis/NIR absorption spectra changes of **1** after titration with ferrocenium hexafluorophosphate.

Table S2. Selected bond lengths and angles of [2-H]/[2-H]⁺ from the computational models, together with analogous data from the crystallographically determined structures of **2**.

Table S3. Selected bond lengths and angles of [3-H]/[3-H]⁺ from the computational models, together with analogous data from the crystallographically determined structures of **3**.

Table S4. Energy and composition of frontier molecular orbitals in the model complexes [2-H]

Table S5. Energy and composition of frontier molecular orbitals in the model complexes [2-H]⁺

Table S6. Energy and composition of frontier molecular orbitals in the model complexes [2-H]²⁺

Table S7. Energy and composition of frontier molecular orbitals in the model complexes [3-H]

Table S8. Energy and composition of frontier molecular orbitals in the model complexes [3-H]⁺

Table S9. Energy and composition of frontier molecular orbitals in the model complexes [3-H]²⁺

Table S10. Major electronic excitations for [2-H] determined by TD-DFT methods using B3LYP/3-21G*

Table S11. Major electronic excitations for [2-H]⁺ determined by TD-DFT methods using B3LYP/3-21G*

Table S12. Major electronic excitations for [3-H] determined by TD-DFT methods using B3LYP/3-21G*

Table S13. Major electronic excitations for [3-H]⁺ determined by TD-DFT methods using B3LYP/3-21G*

Table S1. Crystal data and structure refinement for **2** and **3·CH₂Cl₂**.

Compound	2	3·CH₂Cl₂
formula	C ₉₆ H ₉₄ P ₄ Ru ₂ S ₂	C ₁₀₁ H ₉₈ Cl ₂ P ₄ Ru ₂ S ₂
FW	1637.85	1772.83
<i>T</i> (K)	298(2)	298(2) K
Cryst. syst.	Triclinic	Monoclinic
Space group	P-1	P2(1)/n
<i>a</i> (Å)	11.273(3)	16.3268(17)
<i>b</i> (Å)	18.957(6)	26.119(4)
<i>c</i> (Å)	19.482(6)	20.599(2)
<i>α</i> (°)	91.609(6)	90
<i>β</i> (°)	102.283(6)	103.128(11)
<i>γ</i> (°)	94.418(7)	90
<i>V</i> (Å ³)	4052(2)	8554.5(18)
<i>Z</i>	2	4
<i>D</i> _(calc.) (g cm ⁻³)	1.342	1.377
Absor. coeff. (mm ⁻¹)	0.550	0.587
F(000)	1700	3672
Crystal size (mm ³)	0.10 x 0.09 x 0.08	0.23 x 0.12 x 0.10
<i>θ</i> Range (°)	1.86 to 25.00	1.86 to 28.39
Index ranges	-13 ≤ <i>h</i> ≤ 13,	-21 ≤ <i>h</i> ≤ 21,
	-22 ≤ <i>k</i> ≤ 22,	-34 ≤ <i>k</i> ≤ 34,
	-23 ≤ <i>l</i> ≤ 23	-27 ≤ <i>l</i> ≤ 27
Reflections collected	39683	105393
Independent reflec.	14263 [R _(int) = 0.1261]	21247 [R _(int) = 0.0872]
Data / restr. / param.	14263/19/816	21247/0/1010
Goodness-of-fit / F ²	0.841	1.054
Final R indices [I > 2σ(I)]	R1 = 0.0777, wR2 = 0.1641	R1 = 0.0659, wR2 = 0.1296
	R1 = 0.1843, wR2 = 0.1926	R1 = 0.1119, wR2 = 0.1460
diff. peak and hole	2.905 and -1.832 e. ⁻³	0.765 and -0.393 e. ⁻³

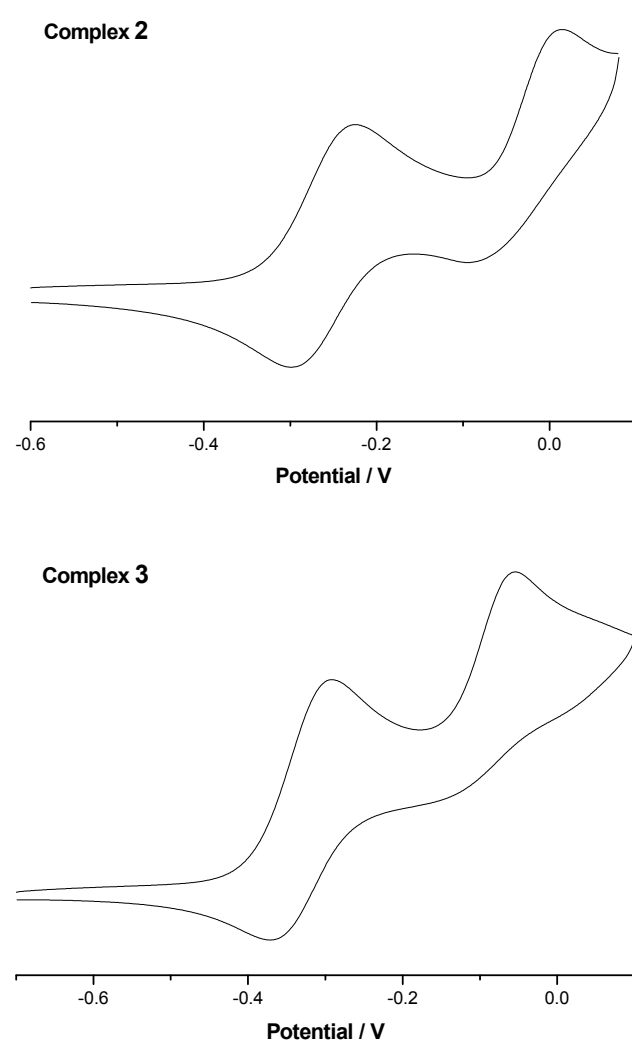


Figure S1. Cyclic voltammograms (CV) of complexes **2** and **3** in $\text{CH}_2\text{Cl}_2/\text{n-Bu}_4\text{NPF}_6$ (0.1 M) at $\nu = 0.1$ V/s.

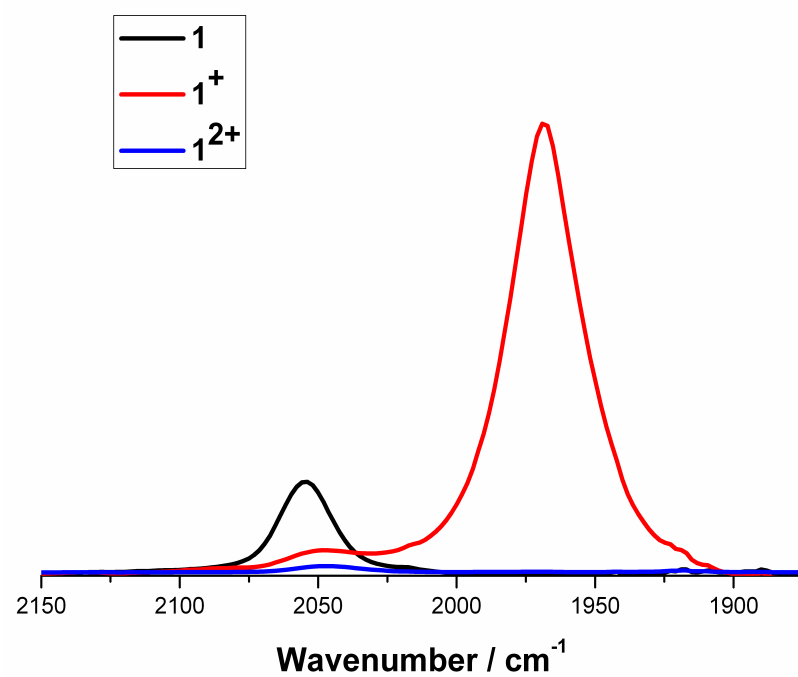


Figure S2. $\nu(\text{C}\equiv\text{C})$ spectra of 1^{n+} ($n = 0-2$) collected during the oxidation titration with ferrocenium hexafluorophosphate ($[\text{FcH}][\text{PF}_6]$).

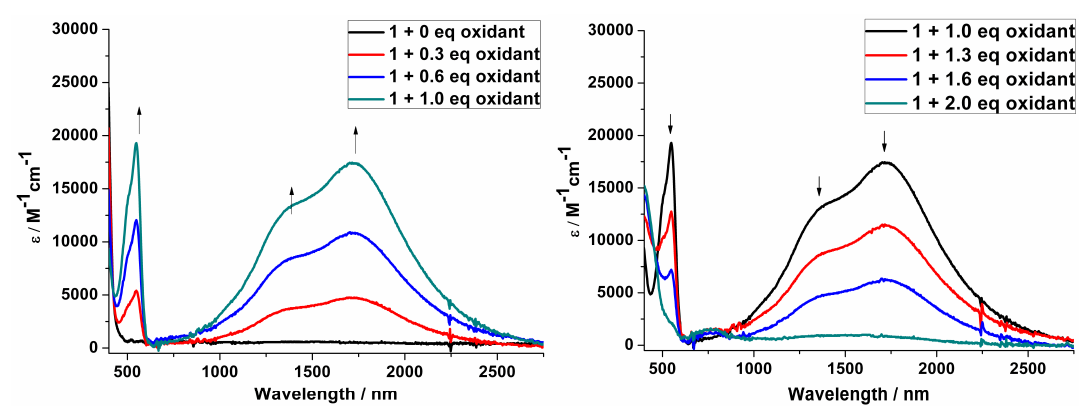


Figure S3. UV/Vis/NIR absorption spectra changes of **2** and **3** after titration with ferrocenium hexafluorophosphate.

Table S2. Selected bond lengths and angles of [2-H]/[2-H]⁺ from the computational models, together with analogous data from the crystallographically determined structures of **2**.^a

Bond distances (Å)			
	2	[2-H]	[2-H] ⁺
Ru(1)-C(37)	1.972(10)	2.01939	1.97621
Ru(1)-P(2)	2.244(3)	2.27798	2.30027
Ru(1)-P(1)	2.247(3)	2.27677	2.29614
Ru(2)-C(60)	2.011(10)	2.01341	1.95863
C(59)-C(60)	1.212(11)	1.22802	1.24281
C(37)-C(38)	1.234(12)	1.22939	1.24094
C(38)-C(39)	1.459(11)	1.42593	1.39714
Ru(2)-P(3)	2.246(3)	2.27902	2.30004
Ru(2)-P(4)	2.244(3)	2.27906	2.30278
C(42)-C(59)	1.439(10)	1.42068	1.38935
Bond angles (°)			
	2	[2-H]	[2-H] ⁺
C(38)-C(37)-Ru(1)	177.4(9)	178.98383	178.50595
C(37)-C(38)-C(39)	169.1(10)	178.90104	177.62154
C(60)-C(59)-C(42)	174.3(10)	179.06653	179.00057
C(59)-C(60)-Ru(2)	170.1(8)	178.54904	175.96723

^a for atom labeling schemes, see ORTEP drawing of compound **2** (Figure 2).

Table S3. Selected bond lengths and angles of **[3-H]**/**[3-H]⁺** from the computational models, together with analogous data from the crystallographically determined structures of **3**.^a

Bond distances (Å)			
	3	[3-H]	[3-H]⁺
Ru(1)-C(37)	2.024(4)	2.01869	1.96993
Ru(1)-P(2)	2.2655(10)	2.27435	2.30177
Ru(1)-P(1)	2.2659(11)	2.27921	2.29569
Ru(2)-C(64)	2.015(4)	2.01843	1.96972
Ru(2)-P(3)	2.2605(12)	2.27965	2.29607
C(37)-C(38)	1.215(5)	1.22847	1.24145
C(38)-C(39)	1.439(5)	1.42592	1.39463
Ru(2)-P(4)	2.2731(11)	2.27428	2.30184
C(42)-C(63)	1.438(5)	1.42597	1.39463
C(63)-C(64)	1.209(5)	1.22849	1.24143
Bond angles (°)			
	3	[3-H]	[3-H]⁺
C(64)-C(63)-C(42)	168.1(4)	175.45320	177.06421
C(63)-C(64)-Ru(2)	167.7(3)	177.17197	178.19118
C(38)-C(37)-Ru(1)	173.6(3)	177.23944	178.19555
C(37)-C(38)-C(39)	172.2(4)	175.70517	177.18415

^a for atom labeling schemes, see ORTEP drawing of compound **3** (Figure 3).

Table S4. Energy and composition of frontier molecular orbitals in the model complexes [**2-H**]

(B3LYP/3-21G*)

MO		eV	(C ₆ H ₂)	(CH ₂ SCH ₂) ₂	(PH ₃) _{2a}	(PH ₃) _{2b}	Cp1	Ru2	(C≡C)2	(C≡C)1	Ru1	Cp2	naph.
217	L+5	-0.04	0	1	21	0	5	0	0	1	71	0	0
216	L+4	-0.21	7	1	12	0	12	1	1	7	54	0	4
215	L+3	-0.27	38	4	2	1	4	4	8	10	13	1	16
214	L+2	-0.51	0	0	0	27	0	50	0	0	0	23	0
213	L+1	-0.85	4	9	1	1	1	1	1	0	2	0	80
212	LUMO	-0.83	0	0	26	0	23	0	0	0	48	0	3
211	HOMO	-4.31	32	1	1	0	1	14	24	16	9	1	1
210	H-1	-4.78	3	5	0	4	0	42	36	1	1	9	0
209	H-2	-5.18	5	3	3	2	6	19	6	21	28	3	4
208	H-3	-5.25	16	12	1	2	1	15	3	8	9	3	31
207	H-4	-5.32	7	8	2	0	2	3	0	17	25	1	35
206	H-5	-5.49	6	40	0	6	0	23	6	1	2	12	4

Table S5. Energy and composition of frontier molecular orbitals in the model complexes [2-H]⁺

(B3LYP/3-21G*)

MOs		eV	(C ₆ H ₂)	(CH ₂ SCH ₂) ₂	(PH ₃) _{2a}	(PH ₃) _{2b}	Cp1	Ru2	(C≡C)2	(C≡C)1	Ru1	Cp2	naph
α-217	α-LUSO+5	-2.82	0	0	14	0	19	1	0	9	55	0	0
β-216	β-LUSO+5	-2.78	0	0	14	0	18	1	0	9	56	0	0
α-216	α-LUSO+4	-2.83	1	0	0	15	0	53	10	0	1	19	0
β-215	β-LUSO+4	-3.02	23	7	0	1	1	3	5	5	2	1	52
α-215	α-LUSO+3	-3.09	10	9	0	1	0	1	1	1	0	0	75
β-214	β-LUSO+3	-3.26	34	7	0	1	1	4	9	7	3	1	34
α-214	α-LUSO+2	-3.43	0	0	26	0	25	0	0	0	49	0	0
β-213	β-LUSO+2	-3.39	0	0	26	0	25	0	0	0	49	0	0
α-213	α-LUSO+1	-3.53	48	4	1	2	1	10	11	9	2	5	7
β-212	β-LUSO+1	-3.48	0	0	0	26	0	48	0	0	0	24	1
α-212	α-LUSO	-3.55	6	1	0	25	0	42	2	1	0	20	3
β-211	β-LUSO	-6.02	30	1	1	1	2	15	21	15	9	3	1
α-211	α-HOSO	-7.23	28	1	2	2	3	12	16	17	14	3	4
β-210	β-HOSO	-7.58	9	6	2	1	5	11	7	13	21	2	23
α-210	α-HOSO-1	-7.65	5	8	0	0	0	0	0	1	2	0	83
β-209	β-HOSO-1	-7.65	8	12	0	1	1	7	4	2	3	1	61
α-209	α-HOSO-2	-7.86	4	70	0	0	0	8	10	1	2	1	5
β-208	β-HOSO-2	-7.87	4	59	0	1	0	14	13	1	2	1	5
α-208	α-HOSO-3	-7.95	5	67	1	0	1	1	1	10	12	0	4
β-207	β-HOSO-3	-7.93	4	56	1	0	2	0	0	14	18	0	4
α-207	α-HOSO-4	-8.09	5	8	4	2	7	15	9	15	30	4	1
β-206	β-HOSO-4	-8.16	3	25	3	1	5	9	4	12	34	1	2
α-206	α-HOSO-5	-8.26	5	12	5	2	9	10	5	10	38	4	1
β-205	β-HOSO-5	-8.22	2	24	1	4	1	36	13	2	6	6	6

Table S6. Energy and composition of frontier molecular orbitals in the model complexes [2-H]²⁺

(B3LYP/3-21G*)

MO		eV	(C ₆ H ₂)	(CH ₂ SCH ₂) ₂	(PH ₃) _{2a}	(PH ₃) _{2b}	Cp1	Ru2	(C≡C)2	(C≡C)1	Ru1	Cp2	naph.
216	L+5	-5.54	9	6	5	1	8	1	0	4	21	0	45
215	L+4	-5.6	0	0	0	15	0	52	10	0	0	21	1
214	L+3	-6.18	0	0	25	0	26	0	0	0	48	0	0
213	L+2	-6.3	2	0	0	24	0	46	0	1	0	26	0
212	L+1	-6.36	52	3	1	3	1	6	14	12	4	1	3
211	LUMO	-8.92	28	1	2	2	3	13	16	16	13	3	4
210	HOMO	-10.02	3	8	0	0	0	0	0	1	1	0	86
209	H-1	-10.33	5	73	1	0	1	4	5	2	4	1	4
208	H-2	-10.41	4	80	0	0	0	2	2	2	2	0	6
207	H-3	-10.58	11	17	3	3	6	17	9	8	17	6	3
206	H-4	-10.93	2	1	0	1	0	5	3	1	2	1	84
205	H-5	-11.01	2	4	4	0	7	2	1	27	53	0	1

Table S7. Energy and composition of frontier molecular orbitals in the model complexes [**3-H**]

(B3LYP/3-21G*)

MO		eV	anth.	C ₆ H ₂	(CH ₂ SCH ₂) ₂	(PH ₃) _{2a}	(PH ₃) _{2b}	Cp1	Ru2	(C≡C) ₂	(C≡C) ₁	Ru1	Cp2
230	L+5	-0.04	0	2	0	12	0	17	1	0	9	56	0
229	L+4	-0.05	0	2	0	0	13	0	56	10	1	1	17
228	L+3	-0.23	55	22	1	1	1	0	6	4	4	5	0
227	L+2	-0.68	0	0	0	27	0	23	0	0	0	50	0
226	L+1	-0.69	0	0	0	0	27	0	50	0	0	0	23
225	LUMO	-1.61	91	1	7	0	0	0	0	0	0	0	0
224	HOMO	-4.28	5	33	1	0	0	1	10	20	20	10	1
223	H-1	-4.92	58	7	6	1	0	2	5	4	7	9	1
222	H-2	-4.96	1	3	4	2	2	4	21	18	19	22	4
221	H-3	-4.99	24	2	3	1	2	2	19	16	12	14	3
220	H-4	-5.27	0	6	3	2	2	3	26	13	13	27	3
219	H-5	-5.46	6	27	63	0	0	0	1	0	0	2	0

Table S8. Energy and composition of frontier molecular orbitals in the model complexes [3-H]⁺

(B3LYP/3-21G*)

MOs		eV	C ₆ H ₂	(CH ₂ SCH ₂) ₂	(PH ₃) ₂ a	anth.	(PH ₃) ₂	Cp1	Ru2	(C≡C)2	(C=C)1	Ru1	Cp2
α-230	α-LUSO+5	-2.78	0	0	0	0	15	0	56	10	0	0	19
β-229	β-LUSO+5	-2.74	0	0	15	0	0	19	0	0	10	56	0
α-229	α-LUSO+4	-2.8	0	0	15	0	0	19	0	0	10	56	0
β-228	β-LUSO+4	-2.99	51	2	1	9	1	1	4	12	12	4	1
α-228	α-LUSO+3	-3.26	55	3	1	9	1	1	3	12	12	3	1
β-227	β-LUSO+3	-3.37	0	0	0	0	26	0	49	0	0	0	25
α-227	α-LUSO+2	-3.42	0	0	0	0	26	0	49	0	0	0	25
β-226	β-LUSO+2	-3.39	0	0	26	0	0	25	0	0	0	49	0
α-226	α-LUSO+1	-3.45	0	0	26	0	0	25	0	0	0	49	0
β-225	β-LUSO+1	-3.84	3	7	0	87	0	0	0	0	0	0	0
α-225	α-LUSO	-3.89	5	7	0	84	0	0	0	1	1	0	0
β-224	β-LUSO	-5.91	29	1	1	5	1	2	11	18	18	11	2
α-224	α-HOSO	-7.01	19	3	1	36	1	2	7	11	11	7	2
β-223	β-HOSO	-7.15	3	6	0	87	0	0	1	1	1	1	0
α-223	α-HOSO-1	-7.28	11	4	1	57	1	1	6	6	6	5	1
β-222	β-HOSO-1	-7.5	11	5	2	1	3	4	21	14	14	21	5
α-222	α-HOSO-2	-7.87	5	54	1	4	1	1	11	9	5	7	2
β-221	β-HOSO-2	-7.86	9	71	0	3	0	0	5	4	3	3	0
α-221	α-HOSO-3	-7.88	8	74	0	3	0	1	1	1	6	6	0
β-220	β-HOSO-3	-7.92	5	51	1	6	0	1	9	7	9	11	1
α-220	α-HOSO-4	-8.1	8	14	3	5	3	5	19	10	10	18	5
β-219	β-HOSO-4	-8.09	3	15	1	1	2	2	27	13	11	20	3
α-219	α-HOSO-5	-8.14	2	11	1	1	3	2	32	15	10	18	4
β-218	β-HOSO-5	-8.15	2	32	2	3	2	3	17	6	9	22	3

Table S9. Energy and composition of frontier molecular orbitals in the model complexes [3-H]²⁺
 (B3LYP/3-21G*)

MO		eV	anth.	C ₆ H ₂	(CH ₂ SCH ₂) ₂	(PH ₃) _{2a}	(PH ₃) _{2b}	Cp1	Ru2	(C≡C) ₂	(C≡C) ₁	Ru1	Cp2
229	L+5	-5.4	0	0	9	0	5	13	20	4	6	34	8
228	L+4	-6.04	1	0	11	0	13	12	26	0	0	22	14
227	L+3	-6.04	0	0	14	0	12	14	22	0	0	26	12
226	L+2	-6.05	48	3	1	15	1	1	4	11	11	4	1
225	L+1	-6.55	10	6	0	77	0	0	1	2	2	1	0
224	LUMO	-8.76	25	2	2	14	2	2	11	15	15	11	2
223	HOMO	-9.77	4	5	0	78	0	1	3	2	2	3	1
222	H-1	-10.32	9	25	3	2	3	5	16	9	9	16	5
221	H-2	-10.43	6	86	0	4	0	0	1	1	1	1	0
220	H-3	-10.51	7	55	1	8	1	2	7	5	4	7	2
219	H-4	-10.88	2	4	2	0	2	3	28	14	14	27	3
218	H-5	-10.9	2	8	2	1	2	4	26	12	13	27	3

Table S10. Major electronic excitations for [**2-H**] determined by TD-DFT methods using B3LYP/3-21G*

Energy (cm ⁻¹)	Wavelength (nm)	Osc. Strength (<i>f</i>)	Major contribs
21351	468	0.0037	HOMO-2→LUMO (11%), HOMO→LUMO (72%)
22839	437	0.0019	HOMO→LUMO+2 (64%)
23647	423	0.0172	HOMO→LUMO+1 (86%)
23704	421	0.0154	HOMO-1→LUMO+2 (66%), HOMO→LUMO+1 (10%)
25911	386	0.0068	HOMO→LUMO+3 (27%), HOMO→LUMO+4 (24%)
26740	374	0.0132	HOMO→LUMO+6 (-13%), HOMO→LUMO+7 (28%)
28449	351	0.0058	HOMO-4→LUMO+3 (20%), HOMO-4→LUMO+4 (18%), HOMO-2→LUMO+3 (-13%), HOMO-2→LUMO+4 (-11%)
29384	340	0.5502	HOMO→LUMO+3 (-37%), HOMO→LUMO+4 (40%)
30004	333	0.0009	HOMO-4→LUMO (11%), HOMO-2→LUMO (20%), HOMO-1→LUMO (29%)
30886	323	0.0793	HOMO-3→LUMO+1 (36%), HOMO→LUMO+6 (22%), HOMO→LUMO+7 (15%)

Table S11. Major electronic excitations for [2-H]⁺ determined by TD-DFT methods using B3LYP/3-21G*

Energy (cm ⁻¹)	Wavelength (nm)	Osc. Strength (<i>f</i>)	Major contribs
7923	1262	0.0028	β-HOSO-5→β-LUSO (-14%), β-HOSO-2→β-LUSO (63%), β-HOSO-1→β-LUSO (-16%)
8414	1188	0.021	β-HOSO-1→β-LUSO (45%), β-HOSO→β-LUSO (43%)
9356	1068	0.073	β-HOSO-4→β-LUSO (-21%), β-HOSO-3→β-LUSO (49%), β-HOSO-1→β-LUSO (-20%)
9936	1006	0.2778	β-HOSO-3→β-LUSO (-29%), β-HOSO-1→β-LUSO (-16%), β-HOSO→β-LUSO (44%)
11421	875	0.0951	β-HOSO-5→β-LUSO (44%), β-HOSO-4→β-LUSO (-23%), β-HOSO-2→β-LUSO (25%)
12209	819	0.044	β-HOSO-5→β-LUSO (34%), β-HOSO-4→β-LUSO (48%), β-HOSO-3→β-LUSO (14%)
13256	754	0.0024	β-HOSO-8→β-LUSO (-13%), β-HOSO-7→β-LUSO (68%), β-HOSO-6→β-LUSO (-13%)
14335	697	0.0098	β-HOSO-7→β-LUSO (22%), β-HOSO-6→β-LUSO (68%)
15502	645	0.0075	β-HOSO-8→β-LUSO (75%), β-HOSO-6→β-LUSO (-12%)
16850	593	0.0042	β-HOSO-9→β-LUSO (85%)
20630	484	0.0025	α-HOSO-4→α-LUSO+2 (17%), α-HOSO→α-LUSO+2 (45%), β-HOSO→β-LUSO+2 (-14%)

Table S12. Major electronic excitations for [**3-H**] determined by TD-DFT methods using B3LYP/3-21G*

Energy (cm ⁻¹)	Wavelength (nm)	Osc. Strength (<i>f</i>)	Major contribs
17318	577	0.0052	HOMO→LUMO (98%)
22053	453	0.0014	HOMO-4→LUMO+1 (-12%), HOMO→LUMO+1 (72%)
23211	431	0.0032	HOMO-3→LUMO (-33%), HOMO-2→LUMO (15%), HOMO-1→LUMO (42%)
23257	429	0.0019	HOMO-3→LUMO (10%), HOMO-2→LUMO (76%)
23665	422	0.0062	HOMO-3→LUMO+2 (-19%), HOMO-2→LUMO+2 (35%)
23689	422	0.008	H HOMO-3→LUMO+1 (33%), HOMO-2→LUMO+1 (21%), HOMO-2→LUMO+2 (-11%)
24238	412	0.0357	HOMO-3→LUMO (52%), HOMO-1→LUMO (28%)
25790	387	0.0043	HOMO-4→LUMO (92%)
26011	384	0.0123	HOMO-5→LUMO (89%)
26216	381	0.001	HOMO→LUMO+4 (55%)
28478	351	0.0991	HOMO→LUMO+3 (74%)

Table S13. Major electronic excitations for [3-H]⁺ determined by TD-DFT methods using B3LYP/3-21G*

Energy (cm ⁻¹)	Wavelength (nm)	Osc. Strength (<i>f</i>)	Major contribs
6038	1656	0.0172	β-HOSO→β-LUSO (100%)
9148	1093	0.1037	β-HOSO-5→β-LUSO (-13%), β-HOSO-3→β-LUSO (-41%), β-HOSO-1→β-LUSO (43%)
10582	945	0.356	β-HOSO-5→β-LUSO (13%), β-HOSO-3→β-LUSO (30%), β-HOSO-1→β-LUSO (54%)
12678	788	0.0236	β-HOSO-5→β-LUSO (73%), β-HOSO-3→β-LUSO (-26%)
13365	748	0.0005	α-HOSO-1→α-LUSO (-23%), α-HOSO→α-LUSO(27%), β-HOSO→β-LUSO+1 (46%)
14494	689	0.0007	β-HOSO-8→β-LUSO (27%), β-HOSO-6→β-LUSO (69%)
14631	683	0.0003	β-HOSO-7→β-LUSO (96%)
15765	634	0.0093	β-HOSO-9→β-LUSO (-14%), β-HOSO-8→β-LUSO (59%), β-HOSO-6→β-LUSO (-21%)
16966	589	0.0062	β-HOSO-9→β-LUSO (76%), β-HOSO-8→β-LUSO (10%)
19405	515	0.0001	β-HOSO-10→β-LUSO (88%)